

Recent star formation in clusters of galaxies: extreme compact starbursts in A539 and A634

D. Reverte, J. M. Vílchez, J.D. Hernández-Fernández and J. Iglesias-Páramo

Instituto de Astrofísica de Andalucía-CSIC, Apdo. 3004, Granada, 18080 Spain

ABSTRACT

We report on the detection of two H α -emitting extreme compact objects from deep images of the Abell 634 and Abell 539 clusters of galaxies at $z \sim 0.03$. Follow up long slit spectroscopy of these two unresolved sources revealed that they are members of their respective clusters showing HII type spectra. The luminosity and the extreme equivalent width of H α + [NII] measured for these sources, together with their very compact appearance, has raised the question about the origin of these intense starbursts in the cluster environment. We propose the compact starburst in Abell 539 resulted from the compression of the interstellar gas of a dwarf galaxy when entering the cluster core; while the starburst galaxy in Abell 634 is likely to be the result of a galaxy-galaxy interaction, illustrating the preprocessing of galaxies during their infall towards the central regions of clusters. The contribution of these compact star-forming dwarf galaxies to the star formation history of galaxy clusters is discussed, as well as a possible link with the recently discovered early-type ultra-compact dwarf galaxies. We note that these extreme objects will be rarely detected in normal magnitude-limited optical or NIR surveys, mainly due to their low stellar masses (of the order of $10^6 M_{\odot}$), whereas they will easily show up in dedicated H α surveys given the high equivalent width of their emission lines.

Subject headings: galaxies: clusters of galaxies, ICM — galaxies: starburst, abundances, star-formation

1. Introduction

The understanding of the role played by the environment on galaxy evolution still remains a major issue. A key aspect to understanding the evolution of galaxies in clusters

is the knowledge of their star formation (SF) history, intimately related to their morphology and gas content. Indeed, it has been reported that the global star formation rates of spiral galaxies located in the innermost regions of nearby and intermediate redshift clusters appear strongly depressed as compared to the results found for similar galaxies at larger clustercentric radii (e.g. Balogh et al. 1998, 2004; Gavazzi et al. 2002; Lewis et al. 2002). Less information is available in the literature with respect to the evolution of the SF activity of the population of dwarf galaxies in clusters. To date, only a handful of works have dealt with the study of the SF activity in the population of star-forming dwarf and irregular galaxies in nearby clusters (e.g. Gallagher & Hunter 1989; Drinkwater & Hardy 1991; Vílchez 1995; Duc et al. 2001; Boselli et al. 2002; Iglesias-Páramo et al. 2003; Lee et al. 2003; Vílchez & Iglesias-Páramo 2003).

Several physical mechanisms have been invoked to explain the influence of the cluster environment on the evolution of star-forming galaxies (see Boselli & Gavazzi 2006). Gas-rich late-type galaxies falling for the first time into the intra-cluster medium (ICM) of a rich cluster can suffer compression of their interstellar medium by ram pressure, triggering star formation bursts; this process can be followed by the stripping of their external gaseous component, thus inducing a quenching of their star formation activity. In addition, gravitational interactions could give rise to different kinds of tidal interactions: with other galaxies, with the cluster potential, “harassment” (Moore et al. 2000). Other important processes include “starvation” of galactic gas component and “preprocessing” of galaxies in falling groups into clusters (Poggianti 2004). Overall, SF activity is expected to be more efficient in high velocity objects at the periphery of the clusters, as shown by numerical simulations (Fujita & Nagashima 1999; Mori et al. 2000). From the observational point of view, it is not yet clear if the SF activity of cluster dwarf irregulars may vary along the clustercentric radius. It seems clear that dwarf galaxies and large spirals should show different responses to the action of cluster tidal fields as a physical consequence of their different mass concentrations (Moore et al. 1999). To date, there is not enough observational information available on the evolution of star-forming dwarf galaxies in clusters, mostly a consequence of the magnitude-limited searches.

Isolated intergalactic HII regions have been recently found in the vicinity of cluster spirals, thus providing evidence for their origin in tidal interactions and from previously processed material (Gerhard et al. 2002; Cortese et al. 2004). Furthermore, a population of intergalactic planetary nebulae (PN) has been reported to exist in Virgo (Freeman et al. 2000; Arnaboldi et al. 2003) and in Coma (Gerhard et al. 2002, 2005) clusters. Obviously the luminosity contrast of the emission lines of HII regions and PN and their relative compactness has allowed them to be detected in nearby clusters, but not in more distant ones given their low luminosities.

A new class of ultra compact dwarf galaxies (UCDGs) in the nearby clusters Fornax (Drinkwater et al. 2000) and Virgo (Jones et al. 2006) has been recently discovered. These galaxies show extremely compact surface brightness profiles and sizes slightly larger than those of stellar clusters, a few tens of pc, with absolute B magnitude $-13 \lesssim M_B \lesssim -11$ (Drinkwater et al. 2004), and typically also present spectra lacking emission-lines. Two explanations for the nature of these galaxies have been proposed: either they are the successors of tidally stripped dEs, or they have originated from merged young massive clusters of tidal origin (Mieske et al. 2006). Up to now, the typical UCDGs reported in clusters do not appear to show recent star formation activity, thus the possibility of analogous star-forming UCDGs in the cluster environment could shed light on the nature and evolution of dwarf galaxies.

A rather unexplored possibility is the search for very compact, actively star-forming dwarf galaxies in clusters. These galaxies should show emission lines with high equivalent widths, as shown by PN and HII regions, though their expected intrinsic luminosity would be much larger than in the cases of PN and HII regions, thus favouring their detection in clusters. Besides the work on Virgo (Gerhard et al. 2002) and Fornax (Drinkwater et al. 2001), there is recent evidence for “missing” compact galaxies in the local field, i.e. galaxies that have been misclassified as stars due to their compactness by standard star-galaxy separation techniques, in the Millennium Galaxy Catalogue (Liske et al. 2006).

In this work we report on the detection and properties of two very compact strong starbursts that have been found associated to the clusters of galaxies Abell 539 and Abell 634. These two objects were discovered by visual inspection of some $H\alpha$ frames covering approximately $1^\circ \times 1^\circ$ on the basis of their compactness and strong $H\alpha$ emission. The parent clusters are approximately at the same distance ($z \approx 0.03$) and show rather different properties: whereas Abell 539 is a rich X-ray luminous cluster, Abell 634 is a poor, disperse cluster, for which only an upper limit in X-ray by ROSAT is available, probably indicating an ongoing galaxy assembling from the cluster outskirts. The adopted heliocentric velocities (velocity dispersions) for A539 and A634 are 8514 km s^{-1} ($\sigma_{A539} = 629 \text{ km s}^{-1}$) and 7945 km s^{-1} ($\sigma_{A634} = 391 \text{ km s}^{-1}$) respectively (Struble & Rood 1999). Thus assuming standard cosmology with $H_0 = 70 \text{ km s}^{-1} \text{ Mpc}^{-1}$, $\Omega_M = 0.3$ and $\Omega_{VAC} = 0.7$, the distances to the clusters adopted throughout this paper are 124.2 (Abell 539) and 115.7 Mpc (Abell 634).

This paper is organized as follows: Section 2 describes the observations and data handling. Section 3 enumerates the main observational properties of the two galaxies and in section 4 we discuss their main properties, origin and evolutionary stage. Finally, in Section 5 we present our conclusions and final remarks about the relative importance of these kinds of objects for the SFR budget of nearby clusters of galaxies.

2. Observations

2.1. Imaging

H α +continuum imaging of the two starburst sources DRP-A539a and DRP-A634a, were obtained with the Wide Field Camera (WFC) attached to the Prime Focus of the 2.5m Isaac Newton Telescope (INT), at the Observatorio de El Roque de los Muchachos (ORM), La Palma, Spain, in December 2002 and 2003, and February 2003. The WFC consists of an array of four thinned AR coated EEV 4k \times 2k devices, plus a fifth used for autoguiding. The pixel scale is 0.33 arcsec pixel⁻¹, which gives a total field of view of about 34' \times 34'. Given the particular arrangement of the detectors, a squared area of about 11' \times 11' is lost in the top right corner of the field. Given the redshift of these objects, an ON-band narrow filter ($\lambda_0 = 6725\text{\AA}$, $\Delta\lambda_{FWHM} = 85\text{\AA}$) to isolate the H α emission and an OFF-band narrow filter ($\lambda_0 = 6563\text{\AA}$, $\Delta\lambda_{FWHM} = 95\text{\AA}$) to measure the continuum emission corresponding to the redshifted H α line were used. At least four different exposures, slightly dithered to remove cosmic rays, were obtained for each position with each filter. The typical seeing of our frames was between 0.8 and 1.5 arcsec except for a few nights of the 2002 run that were around 2 arcsec. Table 1 shows a log of the imaging observations.

Data reduction was performed using the standard software package IRAF¹ following the standard procedure of bias correction, flat-fielding and flux calibration. In order to properly subtract the continuum from the H α emission, the counts of the OFF-band frames were scaled so that the counts of (non saturated) field stars were the same in ON-band and OFF-band frames.

ON-band observations of the spectrophotometric standard stars G191-B2B, PG0934+554, PG0834+546, BD+33 2642, Feige 56 and Feige 67 were taken to perform the flux calibration of our objects. The accuracy of the zero point was 0.05 mag. The photometry of the ON-band and OFF-band sources was performed with the IRAF task qphot, and consisted of circular aperture photometry until convergence of the growth curve was achieved.

Both objects, DRP-A539a and DRP-A634a, appear very compact and much brighter in ON-band than in OFF-band, as shown in figs 1 and 2. While DRP-A539a appears to be an isolated source, a diffuse low surface brightness structure has been detected extending North East from DRP-A634a. Hereafter, the compact source will be referred to as DRP-A634a, whereas the diffuse low surface brightness structure will be named LSB-A634a. Some knotty faint H α emission can be seen at the northern tip of LSB-A634a, which will be referred to

¹Image Reduction and Analysis Facility, written and supported at the National Optical Astronomy Observatories.

as LSB-A634a_knot. Table 2 shows the relevant photometric properties of these objects, as measured from our $H\alpha$ and continuum frames. The luminosities have been corrected for Galactic extinction following Schlegel, Finkbeiner & Davis (1998), and the Cardelli et al. (1989) extinction curve. The $H\alpha+[NII]$ luminosity of LSB-A634a_knot has been estimated assuming that it is located at the same distance as DRP-A634a².

2.2. Spectroscopy

Long slit spectroscopy of DRP-A539a, DRP-A634a and LSB-A634a was obtained with the Alhambra Faint Object Spectrograph and Camera (ALFOSC) attached to the 2.5m Nordic Optical Telescope (NOT) at the ORM on 19th November 2004 and 9th December 2004. Grisms #8 and #14 were used, giving useful spectral ranges of $\lambda 5825\text{--}8350\text{\AA}$ and $\lambda 3275\text{--}6125\text{\AA}$ respectively. The spatial resolution across the slit was $0.19'' \text{ pix}^{-1}$. During the first night, the slit width was set to $1.2''$ resulting in an effective spectral resolution of 7.1 \AA and a 1800 s exposure for each spectral range was obtained for DRP-A634a. The second night was devoted to DRP-A539a and LSB-A634a. Due to an improvement in the weather conditions the slit width was set to $0.4''$, yielding a spectral resolution of 2.8 \AA . A total of 3×1800 s exposures for each spectral range of DRP-A539a were taken with the slit oriented along the parallactic angle. Finally, a 600 s exposure using grism #8 was performed in order to observe the extended emission of LSB-A634a; in this case, the slit was centered on DRP-A634a and was carefully oriented at an angle of 54° (from North to East). Due to an increase in the humidity, this exposure was stopped after 600 s. Table 3 shows the log of spectroscopic observations.

Data reduction was performed using IRAF, following the standard procedure of bias correction, flat-fielding and wavelength and flux calibration. 1-D spectra of DRP-A539a and DRP-A634a were extracted by adding the flux in the spatial sections along the slit which maximize their signal to noise ratios. A total of 10 and 7 pixels were added for DRP-A539a and DRP-A634a respectively. The same procedure was followed to extract a 1-D spectrum for LSB-A634a. As a consequence of its low surface brightness only a faint emission line, spatially corresponding to LSB-A634a_knot, was obtained after adding a total of 21 pixels. As indicated below, this emission line was identified as $H\alpha$.

Both nights were only partially photometric, so an absolute spectrophotometric flux calibration was not attempted. However, the spectrophotometric standard star Hiltner 600 was observed before and after each object with each grism, thus a relative calibration of the

²The possible origins of these objects and their environment will be discussed in Section 3.

spectra in physical units was performed. The spectra corresponding to the red grism were scaled to the blue ones by using the continuum level and the flux of the $[\text{HeI}]\lambda 5876\text{\AA}$ line, present in the blue and red spectra. The scaling factors were found to be ~ 1 within an error bar of $\sim 20\%$. Beyond 7600\AA fringing effects begin to be noticeable and data at longer wavelengths is ineffective. Figures 3 and 4 show the combined (red grism + blue grism) spectra of DRP-A539a and DRP-A634a respectively. Both spectra are dominated by narrow emission lines and show a very faint underlying continuum.

The emission lines were measured with the IRAF task *splot*. The errors of the line fluxes are estimated from the standard deviation of a series of independent repeated measurements, sampling the adjacent continuum for each line. In order to calculate the extinction, the Balmer decrement was computed using the $\text{H}\alpha$, $\text{H}\beta$, $\text{H}\gamma$ and $\text{H}\delta$ line fluxes and compared to their theoretical values (Hummer & Storey 1987). Given the low continuum shown by both objects, no correction for underlying absorption was performed.

Radial velocities were computed from a sigma-weighted average of the redshifts corresponding to the individual emission lines. After applying the heliocentric corrections, values of $v_{rad} = 8940 \pm 40 \text{ km s}^{-1}$ and $8470 \pm 30 \text{ km s}^{-1}$ were found for DRP-A539a and DRP-A634a respectively. The quoted errors correspond to the standard deviations of the velocities derived from individual lines. The measured velocities are offset by about 500 km s^{-1} from the mean heliocentric velocities adopted for the parent clusters. As will be discussed in Sections 4.1 and 4.2, the projected positions of our two objects with respect to the center of the clusters, together with their redshifts, are consistent with their corresponding cluster memberships.

In the spectrum of LSB-A634a.knot, shown in fig. 5, despite the low signal to noise ratio, an emission line was detected at the 3.5σ level. This line, centered at $\lambda = 6747\text{\AA}$ is almost coincident with the wavelength of the $\text{H}\alpha$ line of DRP-A634a. Assuming that this line effectively corresponds to $\text{H}\alpha$, a radial velocity of 8390 km s^{-1} is inferred for LSB-A634a.knot, after correcting for heliocentric relative motions.

In table 4 we present the spectroscopic properties of DRP-A539a and DRP-A634a: reddening corrected line fluxes, reddening coefficient $C(H\beta)$, equivalent widths of $\text{H}\beta$, $\text{H}\alpha$ and $[\text{OII}]$, $\text{H}\beta$ flux, as well as the fluxes of the most prominent emission lines relative to $\text{H}\beta$. As can be seen, the values reported for the $\text{H}\alpha$ equivalent width, though slightly larger than the ones derived from $\text{H}\alpha$ imaging are consistent within the errors.

Table 4 also shows the electron temperatures and oxygen abundances derived using *temden* and *ionic* tasks in the IRAF *nebular* package in STSDAS. Oxygen abundances were derived directly from spectral lines of $[\text{OII}]\lambda 3727$, $[\text{OIII}]\lambda\lambda 4959, 5007$ and using their electron

temperatures from the measurements of [OIII] λ 4363.

3. Results

Figure 6 shows the radial profiles³ of DRP-A539a and DRP-A634a, derived from our sharpest images. The first is marginally different from the typical stellar profile, showing a radius at half maximum $r_{FWHM} \simeq 0.44''$ ($\langle r_{FWHM}^{star} \rangle \simeq 0.39''$). The second is almost indistinguishable from the stellar profile, with $r_{FWHM} \simeq 0.39''$ ($\langle r_{FWHM}^{star} \rangle \simeq 0.38''$). After correcting these profiles for the effect of seeing under the assumption of gaussian PSF⁴, effective (half light) radii of $0.14''$ and $0.09''$ are derived, which correspond to 84 and 32 pc for DRP-A539a and DRP-A634a respectively. These effective radii are lower than most values presented for misclassified compact galaxies in the Millennium Galaxy Catalogue (Liske et al. 2006) and resemble the values typically shown by UCDGs in nearby clusters (Drinkwater et al. 2004).

As concerns LSB-A634a, the length of its major axis from our continuum image was estimated to be $\approx 28''$. At the distance of DRP-A634a this length corresponds to 16 kpc. This value is in good agreement with the dimensions of edge-on disc galaxies. The angular size of the system argues against it being a high redshift object. If, for example, the emission line reported in Section 2.2 was one of the [OIII] lines, the redshift would be $z \approx 0.35$, and the corresponding diameter of the system at such a distance would be 138 kpc, which is highly unlikely for an edge-on galaxy. For the same reason, we can discard the possibility of this system being located at larger distances.

Broad band magnitudes can be derived for DRP-A634a since SDSS frames are available. Aperture photometry corrected for Galactic extinction of DRP-A634a yields $M_{g'} = -15.81$ mag and $M_{r'} = -14.50$ mag. The broad band magnitudes of the composite system LSB-A634a+DRP-A634a were also derived, obtaining $M_{g'} = -17.38$ mag and $M_{r'} = -17.30$ mag. Since DRP-A539a was observed with the *Gunn* r' filter, a value of $M_{r'} \approx -16.07$ mag was estimated for this galaxy. By applying the average $g' - r' = -0.02$ mag of the sample of Ultracompact Blue Dwarf Galaxies of Corbin et al. (2006), a value of $M_{g'} \approx -16.09$

³ We derived the radial profiles using the IRAF task *radprof*. This task fits a point spread function on each star and selected objects in the field through an input coordinate file, deriving a Full Width at Half Maximum of the fitted profile.

⁴ Driver et al. 2005 have reported a slight deviation of a gaussian behaviour when correcting effective radii of galaxies for the effect of seeing in the Millennium Galaxy Catalogue (MGC). For the scope of this work gaussianity behaviour of the PSF is assumed.

is obtained for DRP-A539a. The magnitudes derived for DRP-A539a and DRP-A634a are brighter than those typical of early-type UCDGs in clusters (Mieske et al. 2006). Nevertheless, the Starburst99 model (Leitherer et al. 1999) predicts that the optical magnitudes of an instantaneous burst of star formation can fade by more than 3 magnitudes in about 10^8 yr. These results together with the limits to the sizes of DRP-A539a and DRP-A634a, open the possibility of them being the progenitors of early-type UCDGs recently found in nearby clusters.

The equivalent widths of the most conspicuous Balmer emission lines of our two objects are relatively high: $EW(H\beta)$ (77 and 280\AA for DRP-A539a and DRP-A634a respectively) are in fact above the median value ($\sim 40\text{\AA}$) reported for the sample of HII galaxies of Terlevich et al. (1991) and also for the sample of HI-rich dwarf galaxies in the Hydra cluster of Duc et al. (2001). In addition, $EW(H\alpha+[NII])$ (510 and 1290\AA respectively) are several times larger than the corresponding values of star forming dwarf galaxies reported in other clusters such as Fornax (Drinkwater et al. 2001), Virgo (Boselli & Gavazzi 2002; Boselli et al. 2002), Coma (Iglesias-Páramo et al. 2002) and A1367 (Iglesias-Páramo et al. 2002; Cortese et al. 2006). When comparing with the UCBDs of Corbin et al. (2006) we find that the equivalent width of DRP-A539a is among the typical values of this sample, but DRP-A634a remains an extreme case. The high equivalent widths shown by our two galaxies reveal very strong and young star formation activity. The ages and stellar mass of the recent star formation episodes can be estimated from the luminosities and equivalent widths of the Balmer lines. By assuming an instantaneous burst of star formation, and using Starburst99 (Leitherer et al. 1999) for a Kroupa IMF with $M_{up} = 100 M_{\odot}$ and $M_{low} = 0.5, 0.1 M_{\odot}$ and the Padova AGB tracks, we find that the ages predicted are 5.8 and 4.5 Myr (5 and 4 Myr using Geneva High tracks) for DRP-A539a and DRP-A634a respectively. The corresponding masses which are being converted into stars are 2.0 and $2.2 \cdot 10^6 M_{\odot}$ respectively, with an uncertainty of 15% ⁵. This computation assumes the approximation that all Lyman continuum photons are absorbed by the gas.

Figure 7 shows the luminosity-metallicity relation for dwarf galaxies (after Pilyugin, Vílchez, & Contini 2004), including the points for DRP-A539a and DRP-A634a, with $M_B = -15.60$ mag and -15.89 mag respectively. B absolute magnitudes have been obtained from $M_{g'}$ after applying the correction term $g' - B = -0.21$, as reported by Fukugita et al. (1995) for late-type dwarf galaxies. The two points follow the mean relation reported for nearby dwarf galaxies and remain far from the locus occupied by typical tidal dwarf galaxies (TDG) (see review by Kunth & Östlin 2000 and references therein). In figure 7, the point corresponding to

⁵The derived values for the age and stellar mass of the burst are the nominal values obtained from the measured imaging $H\alpha$ flux and corresponding error (derreddening error is included).

the integrated system LSB-A634a+DRP-A634a appears to separate from the luminosity-metallicity relation by more than 1 mag, being too luminous for the metallicity derived for DRP-A634a (table 4).

4. Discussion

4.1. DRP-A539a

Figure 8 shows the optical DSS (Palomar Digitalized Sky Survey) frame of the inner region of the cluster A539. Contours corresponding to the X-ray emission⁶ and to the surface density of galaxies (from 2MASS) of A539 are overlaid. It can be seen that the maxima of surface density of galaxies and X-ray are coincident. The X-ray luminosity of A539 is $6.7 \times 10^{44} \text{ erg s}^{-1}$ (White, Jones & Forman 1997). Its velocity dispersion was estimated to be 629 km s^{-1} , thus giving a total dynamical mass for the cluster of $32 \times 10^{13} M_{\odot}$ (Struble & Rood 1999). The projected distance of DRP-A539a from the center of A539 is 300 kpc, which corresponds to $0.2 \times r_{200}$. This short distance together with the measured radial velocity of DRP-A539a, ensures that this object is well within the region defined by the caustic of the cluster (see Figure 2 of Rines et al. 2003⁷).

The existence of such an active star forming object at such a short distance from the center of a cluster is unusual and opens several questions about its nature and origin. One possibility is that this object could be a tidal dwarf galaxy, resulting from a galaxy-galaxy interaction. These kinds of objects have been previously reported in different environments such as clusters (Duc et al. 1999, 2000; Iglesias-Páramo et al. 2003), groups (Iglesias-Páramo & Vílchez 2001; Mendes de Oliveira et al. 2004) or just pairs of interacting galaxies (Mirabel, Dottori & Lutz 1992; Duc et al. 2000). TDGs originate out of the tidal features resulting during the interaction, and under certain conditions they can escape the potential well of the parent galaxy and evolve independently (Elmegreen, Kaufman & Thomasson 1993). A visual inspection of the ON-band and OFF-band frames shows no signatures of galaxy-galaxy interactions around DRP-A539a. The closest galaxy is 2MASX J05165377+0619216, an S0 galaxy whose radial velocity is $v = 8063 \text{ km s}^{-1}$, located at a projected distance of 32 arcsec (about 18 kpc). We analyzed the isophotes of this galaxy and did not find any

⁶From 0.4-2.4 Kev ROSAT map.

⁷In the particular case of A539, the caustic appears well defined and any possible contamination is low. However, these authors remark that although the caustic separates cluster members from foreground and background galaxies in a more efficient way than the velocity sigma clipping, still some interlopers may lie within the caustics.

distortion or abnormal twist of the isophotes that could be taken as a signature of interaction. Moreover, no diffuse emission was detected around this galaxy in the direction of DRP-A539a. In addition, as shown in Figure 7, DRP-A539a follows the mean luminosity-metallicity relation derived for a large sample of dwarf galaxies. Based on these arguments, we can discard DRP-A539a as being a TDG.

Another possibility is that DRP-A539a is the product of ICM-induced efficient star formation in gas clouds drifting into the cluster (Bekki & Couch 2003). In this scenario the star formation activity results from the compression of molecular clouds stripped from spiral galaxies through galaxy-galaxy or galaxy-tidal field interactions. Isolated intra-cluster HII regions have already been reported in the Virgo cluster (Gerhard et al. 2002; Cortese et al. 2004). However, these HII regions are more than one order of magnitude less luminous than DRP-A539a. It should be noted that the objects studied in Cortese et al. (2004) are located close to the two bright spirals VCC 836 and VCC 873, which are probably their progenitors. Nonetheless, DRP-A539a does not appear to be associated to any gas-rich bright galaxy, suggesting that either the parent molecular cloud is the result of an ancient episode of gas stripping, where the stripped galaxy is already far away, or rather we are facing a star forming dwarf galaxy (SFDG) falling for the first time into the cluster core. Theoretical models predict that SFDGs lose their external gas very rapidly when they enter the cluster potential well, due to the ram pressure exerted by the ICM (Mori et al. 2000) and also, according to Bekki & Couch (2003), the timescale for transformation of gas into stars due to ICM pressure is of the order of 10 Myr; for this reason we argue that DRP-A539a is in the very early stages of the infall process.

4.2. DRP-A634a

Figure 9 shows the optical DSS frame of the cluster A634 with the overlaid contours corresponding to the surface density of galaxies derived from 2MASS. This cluster is not detected in X rays by the ROSAT mission, so an upper limit of $6 \cdot 10^{41}$ erg s^{-1} is adopted for its X-ray luminosity. The non detection of X-ray emission means that this cluster is probably in the process of formation and therefore a virialized core is not yet in place. Nevertheless, the smoothed surface density contours from 2MASS show a dense central aggregate of galaxies showing the galaxy cluster location and shape. We must note that the cluster center as indicated by the 2MASS-contours, $\alpha = 08:15:08$, $\delta = +58:14:58$, is about 12 arcmin away from the center quoted in Struble & Rood (1999). Hereafter, for our dynamical considerations and being conservative, we have adopted the center of the cluster inferred by the 2MASS contours. The heliocentric velocity measured for DRP-A634a differs from the

cluster heliocentric velocity by $1.34 \times \sigma_{A634}$ km s⁻¹, and this object is located at a projected distance of 398 kpc from the cluster center. Both values, heliocentric velocity and projected distance, would place DRP-A634a within the caustic of every galaxy cluster presented in Rines et al. (2003), at the 2σ confidence level⁸; Especially in the case of A194, a cluster presenting velocity dispersion and extension in the sky very similar to those of A634. The non detection in X-ray of A634 together with the substantial distance of DRP-A634a to the cluster center, may weaken the hypothesis that the strong star formation activity shown by this object could be the result of compression of molecular clouds due to the pressure exerted by the ICM. Nonetheless, we must bear in mind that the lack of detection of X-Ray emission in A634 does not necessarily mean it is devoid of a significant ICM.

The comparable radial velocities measured for DRP-A634a and LSB-A634a, and their close position in the sky could be indicative of both objects being physically related. The optical morphology of the LSB-A634a+DRP-A634a system may suggest an edge-on, late-type, low surface brightness galaxy, with an off-center very bright knot accounting for most of the optical light. In this scenario, would this system be anywhere close to the Tully-Fisher (TF) relation? To answer this question, first we have assumed that the difference between the radial velocities of DRP-A634a and LSB-A634a.knot provides an estimation of the internal velocity of the system, giving $2 V_{max} \approx 80$ km s⁻¹. Secondly, we have applied the results of Pierini & Tuffs (1999), who derived the TF relation for a sample including dwarf star-forming galaxies from the Virgo Cluster Catalogue in the K' band. The $M_{K'}$ magnitude of the system was derived from the M_B magnitude (see sect. 3) making use of: 1) the average $(B - K)$ colour for the Virgo sample of 57 (Sdm - Sd/Sm to Im/BCD) galaxies⁹: $(B - K) \simeq 2.85$; and 2) the mean colour, $(B - K_s) \simeq 2.20$, obtained for the sample of BCDs from Noeske et al. (2003). Taking the average value of both results, $\langle (B - K) \rangle = 2.53 \pm 0.33$, we found $M_{K'} = -19.70 \pm 0.35$ mag for the system LSB-A634a+DRP-A634a. Applying the fit of Pierini & Tuffs (1999) (see their figure 6) to our value of V_{max} , their TF relation predicts $M_{K'} = -16.89$ mag, nearly 3 mag fainter than the value of $M_{K'}$ estimated above for the whole system. In the optical, several papers on the TF relation for low luminosity galaxies have appeared recently. The TF relation for local discs and irregular galaxies from Ziegler et al. (2002) would predict a value of $M_B \sim -15$ mag for our $V_{max} \approx 40$ km s⁻¹, about 2 mag fainter than the value measured for our system. According to Swaters (1999) (figure 13, page 117), galaxies with absolute magnitudes fainter than $M_{r'} \simeq -18$ systematically fall below

⁸ In the case the cluster center quoted by Struble & Rood (1999) is adopted, the corresponding projected distance would amount to 16 kpc and DRP-A634a will be a cluster member at a higher confidence level.

⁹ The GOLDmine database (Gavazzi et al. 2003b) was used to derive these data - <http://goldmine.mib.infn.it/>

a straight line TF relation. This fact has been highlighted by McGaugh (2000) pointing out the different evolutionary stage of gas-rich dwarfs with respect to spiral discs. More recently Schombert (2006) concluded that dwarf galaxies form a distinct sequence, being more diffuse than disc galaxies. To summarize, the predictions of the TF relation for galaxies with internal velocity of order $V_{max} \approx 40 \text{ km s}^{-1}$ yield luminosity values much fainter than that determined here for this system. On the other side, as mentioned in sect. 3 this integrated system separates from the luminosity-metallicity relation being too luminous for its metallicity. According to these findings, the object formed by LSB-A634a+DRP-A634a is not proven to be a single galaxy.

Even though the LSB-A634a+DRP-A634a system is not likely to be a single galaxy, still both objects could be physically related. Under this assumption, we propose that the strong star formation activity shown by DRP-A634a is the result of the encounter between these objects. In fact, examples of recent star formation bursts associated to small groups of galaxies which are falling into a cluster have already been reported in the literature (Sakai et al. 2002; Gavazzi et al. 2003a; Cortese et al. 2006), and are thought to be associated to the so-called preprocessing of galaxies before entering the cluster environment. This mechanism could account for a non negligible fraction of the evolution of galaxies in dense environments. Further observations of this intriguing system are needed in order to fully understand its nature and evolutionary state.

5. Conclusions

We have reported two examples of extreme star forming objects in nearby clusters with different properties and at different evolutionary phases. The observations show that albeit they do not share the same origin, both compact and young starbursts show a very intense star formation activity, even when compared to similar objects in other nearby clusters or in less dense environments.

The origin of the two starbursts reported in this paper are probably associated to different physical mechanisms: DRP-A539a is directly associated to the dense and hot ICM which compresses intergalactic clouds and induces star formation episodes in a short timescale, before ram pressure is able to sweep the external gas. The case of DRP-A634a can be related to the so-called “preprocessing” of galaxies before they enter the cluster environment. In this case, the aggregates of galaxies whose final fate is to fall into the cluster inner regions, are the environments where secondary evolution is taking place.

Two questions arise from these considerations: what is the relative importance of such

compact and extreme starbursts with respect to the global SFR of nearby clusters? and, is there any evolutionary link between them and the early-type ultracompact dwarf galaxies already reported in the literature? (Drinkwater et al. 2004) To answer the first question, a detailed search based on $H\alpha$ surveys is required. We note that an extensive spectroscopic survey of Abell 539 devoted to studying the star formation in cluster galaxies has been carried out by Rines et al. (2005), but DRP-A539a was not selected there because their sample of galaxies was NIR-magnitude limited. The same would have happened with DRP-A634a if the cluster A634 had been surveyed under the same conditions. These non detections are naturally explained by the fact that these objects are dwarfs and very young. However, they show up very easily in wide field $H\alpha$ imaging surveys despite their size and small stellar content. These kinds of surveys are required to carry out a detailed census of compact starbursts in clusters of galaxies. In this way, their relative contribution to the total SFR budget of nearby clusters will definitely be determined. As concerns the second question, several explanations have already been proposed for the origin of UCDGs (see Jones et al. 2006 for an interesting review), although the discussion remains open. We propose that compact and strong starbursts like the ones presented in this paper could evolve to early-type dwarf galaxies after cessation of star formation and, if stripping is efficient as the galaxy approaches the innermost regions of the cluster, become UCDGs like the ones reported in Virgo and Fornax clusters. A complete census of compact starbursts in clusters, with accurate projected positions and surface densities will also help to answer this question.

We thank the anonymous referee for his/her useful comments and suggestions. We also want to thank Steve Donegan for his careful revision of the english expression in this paper. The data presented in this paper were obtained using ALFOSC, which is owned by the Instituto de Astrofísica de Andalucía (IAA) and operated at the Nordic Optical Telescope under agreement between IAA and the NBIfAFG of the Astronomical Observatory of Copenhagen. This article is based on observations made with the Isaac Newton Telescope (INT) operated on the island of La Palma (Canary Island) by the Isaac Newton Group (ING) in the spanish Observatorio del Roque de los Muchachos. This research has made use of the NASA/IPAC Extragalactic Database (NED) which is operated by the Jet Propulsion Laboratory, California Institute of Technology, under contract with the National Aeronautics and Space Administration. This research has made use of the GOLDMine Database (Gavazzi et al. 2003b). This publication makes use of data products from the Two Micron All Sky Survey, which is a joint project of the University of Massachusetts and the Infrared Processing and Analysis Center/California Institute of Technology, funded by the National Aeronautics and Space Administration and the National Science Foundation. This work has been partially funded by the projects AYA2004-08260-C03-02, of spanish PNAYA, and TIC114 of the Junta

de Andalucía.

A. Appendix material

REFERENCES

- Arnaboldi, M., Freeman, K.C., Okamura, S., et al. 2003, *AJ*, 125, 514
- Balogh, M. L., Schade, D., Morris, S. L., Yee, H. K. C., Carlberg, R. G., and Ellingson, E. 1998, *ApJ*, 504, L75
- Balogh, M. L., Baldry, Ivan K., Nichol, R., Miller, C., Bower, R., and Glazebrook, K. 2004, *ApJ*, 615, L101
- Bekki, K., and Couch, W. J. 2003, *ApJ*, 596, L13
- Boselli, A., and Gavazzi, G. 2002, *A&A*, 386, 124
- Boselli, A., Iglesias-Páramo, J., Vílchez, J. M., and Gavazzi, G. 2002, *A&A*, 386, 143
- Boselli, A., and Gavazzi, G. 2006, *PASP*, 118, 517
- Cardelli, J. A., Clayton, G. C., and Mathis, J. S. 1989, *ApJ*, 345, 245
- Corbin, M. R., Vacca, W. D., Cid Fernandes, R., Hibbard, J. E., Somerville, R. S., Windhorst, R. A. accepted for publication in *ApJ*, astro-ph/0607280
- Cortese, L., Gavazzi, G., Boselli, A., and Iglesias-Páramo, J. 2004, *A&A*, 416, 119
- Cortese, L., Boselli, A., Buat, V., Gavazzi, G., Boissier, S., Gil de Paz, A., Seibert, M., Madore, B. F., and Martin, D. C. 2006, *ApJ*, 637, 242
- Drinkwater, M., and Hardy, E. 1991, *AJ*, 101, 94
- Drinkwater, M. J., Jones, J. B., Gregg, M. D., and Phillipps, S. 2000, *Publications of the Astronomical Society of Australia*, 17, 227
- Drinkwater, M. J., Gregg, M. D., Holman, B. A., and Brown, M. J. I. 2001, *MNRAS* 326, 1076
- Drinkwater, M. J., Gregg, M. D., Couch, W. J., Ferguson, H. C., Hilker, M., Jones, J. B., Karick, A., and Phillipps, S. 2004, *PASA*, 21, 375
- Driver, S. P., Liske, J., Cross, N. J. G., De Propris, R., and Allen, P. D. 2005, *MNRAS*, 360, 81

- Duc, P. A., Papaderos, P., Balkowski, C., Cayatte, V., Thuan, T. X., and van Driel, W. 1999, *A&ASS*, 136, 539
- Duc, P. A., Brinks, E., Springel, V., Pichardo, B., Weillbacher, P., and Mirabel, I. F. 2000, *AJ*, 120, 1238
- Duc, P. A., Cayatte, C., Balkowski, C., Thuan, T. X., Papaderos, P., and van Driel, W. 2001, *AJ*, 369, 763
- Elmegreen, B.G., Kaufman, M., and Thomasson, M. 1993, *ApJ*, 412, 90
- Freeman, K. C., Arnaboldi, M., Capaccioli, M., Ciardullo, R., Feldmeier, J., Ford, H., Gerhard, O., Kudritzki, R., Jacoby, G., Méndez, R. H., and Sharples, R. 2000, *ASPC*, 197, 389
- Fujita, Y., and Nagashima, M. 1999, *ApJ*, 516, 619
- Fukugita, M., Shimasaku, K., and Ichikawa, T. 1995, *PASP*, 107, 945
- Gallagher, J. S., III, and Hunter, D. A. 1989, *AJ*, 98, 806G
- Gavazzi, G., Boselli, A., Pedotti, P., Gallazzi, A., and Carrasco, L. 2002, *A&A*, 396, 449
- Gavazzi, G., Cortese, L., Boselli, A., Iglesias-Páramo, J., Vílchez, J. M., and Carrasco, L. 2003a, *ApJ*, 597, 210
- Gavazzi, G., Boselli, A., Donati, A., Franzetti, P., and Scodreggio, M. 2003b, *A&A*, 400, 451
- Gerhard, O., Arnaboldi, M., Freeman, K. C., and Okamura, S. 2001, *AJ*, 581, 109
- Gerhard, O., Arnaboldi, M., Freeman, K. C., Kashikawa, N., Okamura, S., and Yasuda, N. 2005, *ApJ*, 621, L93
- Hummer, D. G., and Storey, P. J. 1987 *MNRAS*, 224, 801
- Iglesias-Páramo, J., and Vílchez, J. M. 2001, *ApJ*, 550, 204
- Iglesias-Páramo, J., Boselli, A., Cortese, L., Vílchez, J. M., and Gavazzi, G. 2002, *A&A*, 384, 383
- Iglesias-Páramo, J., van Driel, W., Duc, P. A., Papaderos, P., and Vílchez, J. M. et al 2003, *A&A*, 406, 453
- Jones, J. B, Drinkwater, M. J., Jurek, R., Phillips, S., Gregg, M. D., Bekki, K., Couch, W. J., et al. 2006, *AJ*, 131, 312

- Kunth, D., and Östlin, G. 2000, *A&ARv*, 10, 1
- Lee, H., McCall, M. L., and Richer, M. G. 2003, *AJ*, 125, 2975
- Leitherer, C., Shaerer, D., Goldader, J. D., González-Delgado, R. M., et al 1999, *AJSS*, 123, 3
- Lewis, I., Balogh, M., De Propris, R., Couch, W., Bower, R., Offer, A., Bland-Hawthorn, J., Baldry, I. K., et al. 2002, *MNRAS*, 334, 673
- Liske, J., Driver, S. P., Allen, P. D., Cross, N. J. G., and De Propris, R., submitted to *MNRAS*, astro-ph/0604211
- Noeske, K. G., Papaderos, P., Cairós, L. M., and Fricke, K. J. 2003, *A&A*, 410, 481
- McGaugh, S. 2000, *Bulletin of the American Astronomical Society*, 32, 1496
- Mendes de Oliveira, C., Cypriano, E. S., Sodr e Jr., L., and Balkowski, C. 2004, *ApJ*605, L17
- Mieske, S., Hilker, M., Infante, L., and Jord an, A. 2006, *AJ*, 131, 2442
- Mirabel, I.F., Dottori, H., and Lutz, D. 1992, *A&A*, 256, L19
- Moore, B., Lake, G., Quinn, T., and Stadel, J. 1999, *MNRAS*, 304, 465
- Moore, B., Quilis, V., and Bower, R. 2000, *ASPC*, 197, 363
- Mori, M., and Burkert, A. 2000, *ApJ*, 538, 559
- Pierini, D., and Tuffs, R. J. 1999, *A&A*, 343, 751
- Piluygin, L. S., V lchez, J. M., and Contini, T. 2004, *A&A*, 425, 849
- Poggianti, B. 2004, *Baryons in Dark matter halos*. Novigrad, Croatia, 5-9 Oct 2004. Proceedings of Science, <http://pos.sissa.it>, p.104.1
- Rines, K., Geller, M., Kurtz, M., and Diaferio, A. 2003, *AJ*, 126, 2152
- Rines, K., Geller, M., Kurtz, M., and Diaferio, A. 2005, *AJ*, 130, 1482
- Sakai, S., Kennicutt, R. C., van der Hulst, J. M. and Moss, C. 2002, *ApJ*, 578, 842
- Schlegel, D. J., Finkbeiner, D. P., and Davis, M. 1998, *ApJ*, 500, 525
- Schombert, J. M. 2006, *AJ*, 131, 296

- Struble, M. F., and Rood, H. J. 1999, *ApJS*, 125, 35
- Swaters, R. A. 1999, Ph.D. Thesis. Gröningen University.
- Terlevich, R., Melnick, J., Masegosa, J., Moles, M., and Copetti, M. V. F. 1991, *A&AS*, 91, 285
- Thuan, T. X., and Martin, G. E. 1981, *ApJ*, 247, 823
- Verdes-Montenegro, L., Del Olmo, A., Iglesias-Páramo, J., Perea, J., Vílchez, J. M., Yun, M. S., and Hutchmeier, W. K. 2002, *A&A*, 396, 815
- Vílchez, J. M. 1995, *AJ*, 110, 1090
- Vílchez, J. M., and Iglesias-Páramo, J. 2003, *ApJS*, 145, 225
- White, D. A., Jones, C., and Forman, W. 1997, *MNRAS*, 292, 419
- Ziegler, B. L., et al. 2002, *ApJ*, 564, L69

Table 1. Imaging observations log.

Object	Filter	Exp. time (s)	Date
DRP-A539a	ON	5×600	3 Dec. 2002
	ON	1×1200	3 Dec. 2002
	ON	1200	4 Dec. 2002
	OFF	2×1200	28 Feb. 2003
	OFF	5×600	28 Feb. 2003
	OFF	1200	4 Dec. 2002
	r'	3×300	3 Dec. 2002
DRP-A634a	ON	1200	9 Feb. 1999
	ON	2×1200	26 Feb. 2003
	ON	3×400	28 Feb. 2003
	OFF	1200	9 Feb. 1999
	OFF	2×1200	26 Feb. 2003
	OFF	4×400	28 Feb. 2003

Table 2. Basic photometric properties of DRP-A539a and DRP-A634a measured from our H α and continuum frames: (1) Object Id; (2) R.A.; (3) Dec.; (4) H α + [NII] luminosity corrected for Galactic extinction; (5) H α + [NII] equivalent width

Object	R.A. (J2000)	Dec. (J2000)	$L(\text{H}\alpha + [\text{NII}])$ ($10^{40} \text{ erg s}^{-1}$)	$\text{EW}(\text{H}\alpha + [\text{NII}])$ (\AA)
DRP-A539a	05:16:51.7	+06:19:32.1	1.27 ± 0.03	430 ± 60
DRP-A634a	08:13:55.6	+58:02:32.4	2.38 ± 0.21	1010 ± 230
LSB-A634a_knot	08:13:57.0	+58:02:42.5	1.03 ± 0.25	65 ± 23
LSB-A634a+DRP-A634a			3.4 ± 0.4	190 ± 40

Table 3. Spectroscopy Observations log.

Object	Date	Spect. Range (Å)	Exp. Time (s)	Slit width (arcsec)	Position angle [†] (deg)
DRP-A634a	2004-11-19	3700-6100	1 × 1800	1.2	245.5
DRP-A634a	2004-11-19	6000-8000	1 × 1800	1.2	235.5
DRP-A539a	2004-12-09	3700-6100	3 × 1800	0.4	336.4, 356.4, 15.4
DRP-A539a	2004-12-09	6000-8000	3 × 1800	0.4	312.7, 323.1, 30.4
LSB-A634a+DRP-A634a	2004-12-09	6000-8000	1 × 600	0.4	54.0

Note. — [†]Position angle (measured from North to East) corresponds for every value on the table to the Parallaxic Angle except the last exposure.

Table 4. Reddening corrected line intensities of the Objects DRP-A539a and DRP-A634a relative to $H\beta=1000$. The reddening coefficient $C(H\beta)$, electron temperatures, oxygen abundances, as well as the $H\beta$ flux and the equivalent width and for $H\beta$, $H\alpha$ and $[OII]$ are quoted. $H\beta$ flux has been corrected for Galactic and intrinsic extinction using the extinction law $R = 3.1$ and their $C(H\beta)$

Line	λ (\AA)	f_λ	DRP-A539a	DRP-A634a
[OII]	3727	0.28	1058 ± 7	375 ± 17
[NeIII]	3868	0.24	522 ± 14	419 ± 80
H ϵ	3889	0.24	210 ± 19	112 ± 15
H δ	3970	0.22	320 ± 30	258 ± 17
[SII]	4068	0.20	77 ± 15	—
H δ	4101	0.19	268 ± 15	171 ± 22
H γ	4340	0.13	513 ± 10	473 ± 21
[OIII]	4363	0.13	70 ± 20	202 ± 16
HeI	4471	0.10	—	53 ± 13
[ArIV]	4711	0.04	—	59 ± 14
H β	4861	0.00	1000 ± 16	1000 ± 10
[OIII]	4959	-0.04	1869 ± 7	2740 ± 14
[OIII]	5007	-0.05	5280 ± 40	8272 ± 10
HeI	5876	-0.26	73 ± 8	105 ± 10
H α	6563	-0.37	2827 ± 5	2789 ± 5
[NII]	6584	-0.37	47 ± 5	27 ± 5
HeI	6678	-0.38	—	29 ± 5
[SII]	6717	-0.39	112 ± 10	46 ± 5
[SII]	6731	-0.39	130:	29 ± 5
HeI	7065	-0.43	—	58 ± 7
[ArIII]	7135	-0.44	—	85 ± 9
$C(H\beta)$			0.27	0.47
$T_e([OIII])$	(K)		12800 ± 1500	16800 ± 700
$T_e([OII])$	(K)		11900 ± 1000	14800 ± 500
$12+\log(O^+/H^+)$			7.65 ± 0.14	6.75 ± 0.06
$12+\log(O^{++}/H^+)$			7.93 ± 0.14	7.83 ± 0.05
$12+\log(O/H)$			8.12 ± 0.14	7.87 ± 0.06
$F(H\beta)$	$(10^{-15} \text{ erg cm}^{-2} \text{ s}^{-1})$		4.21 ± 0.09	8.75 ± 0.08
$EW(H\beta)$	(\AA)		77 ± 17	280 ± 90
$EW(H\alpha)$	(\AA)		510 ± 90	1290 ± 120
$EW([OII])$	(\AA)		70 ± 15	110 ± 40

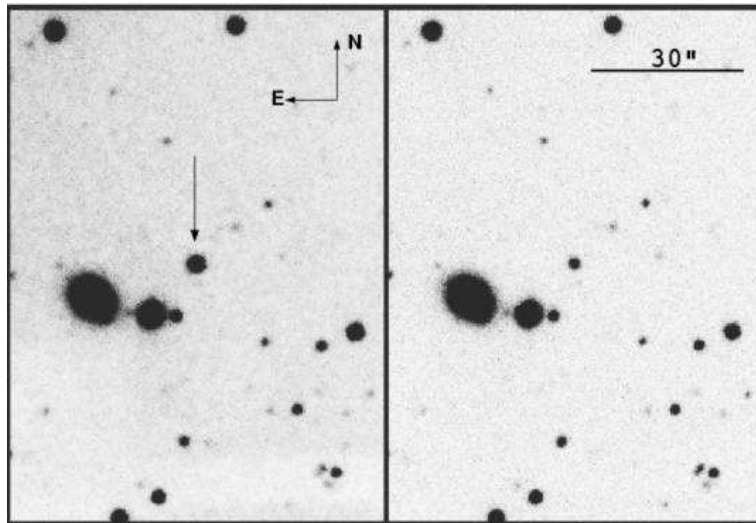


Fig. 1.— ON-band ($H\alpha$ - left) and OFF-band (red continuum - right) images of DRP-A539a region. The arrow indicates the position of the object.

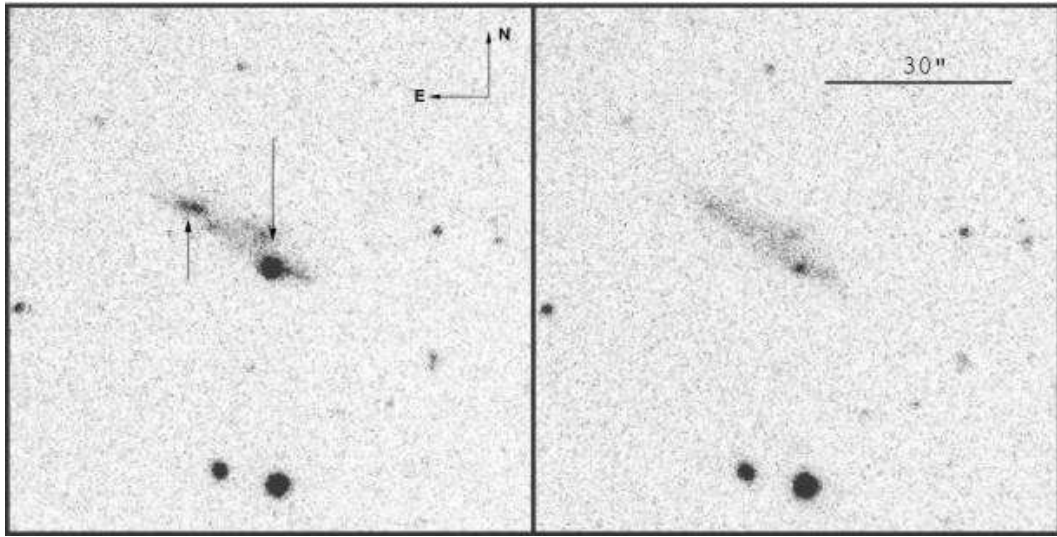


Fig. 2.— ON-band ($H\alpha$ - left) and OFF-band (red continuum - right) images of DRP-A634a region. The downward arrow indicates the position of DRP-A634a. The upward arrow points to LSB-A634a.knot . The low surface brightness structure apparent in the right panel is LSB-A634a.

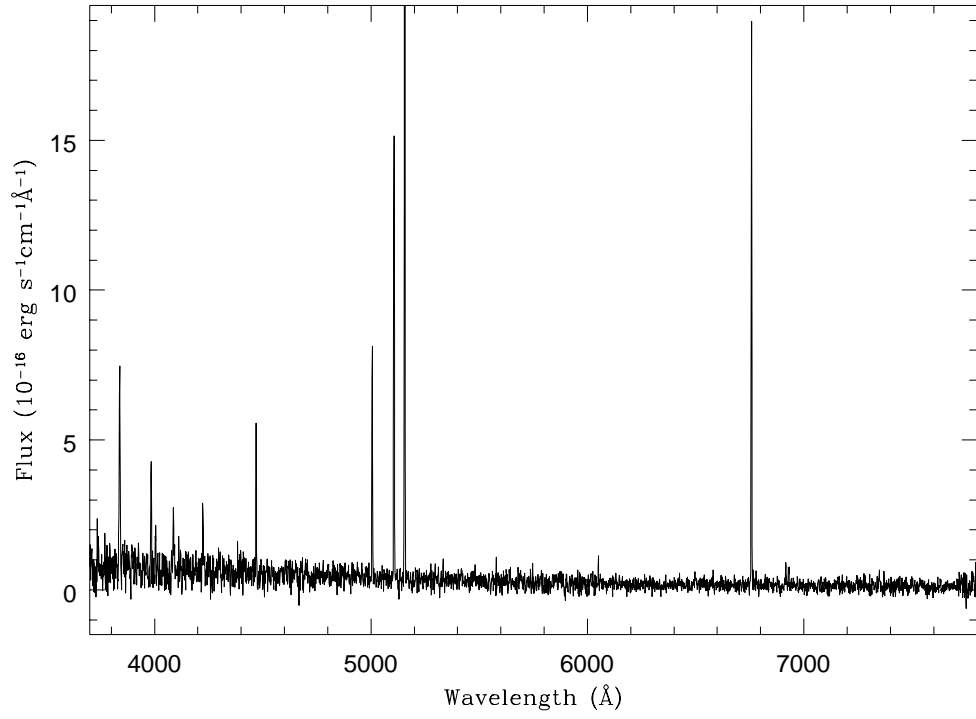


Fig. 3.— Combined spectrum of DRP-A539a scaled to $[\text{OIII}]\lambda 4959 \text{ \AA}$.

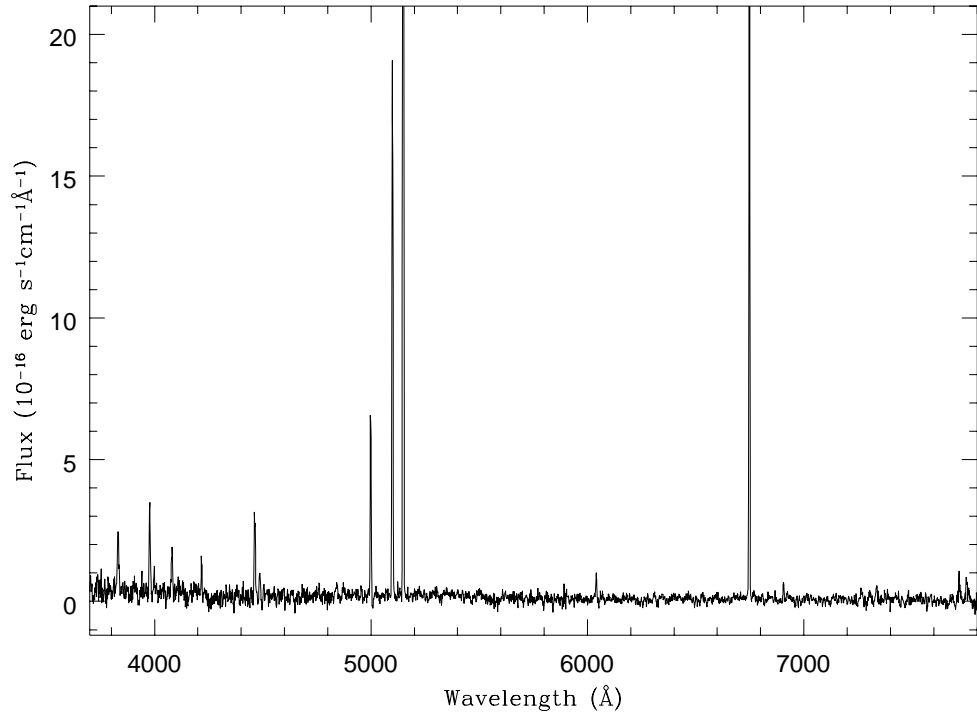


Fig. 4.— Same as Figure 3 for DRP-A634a.

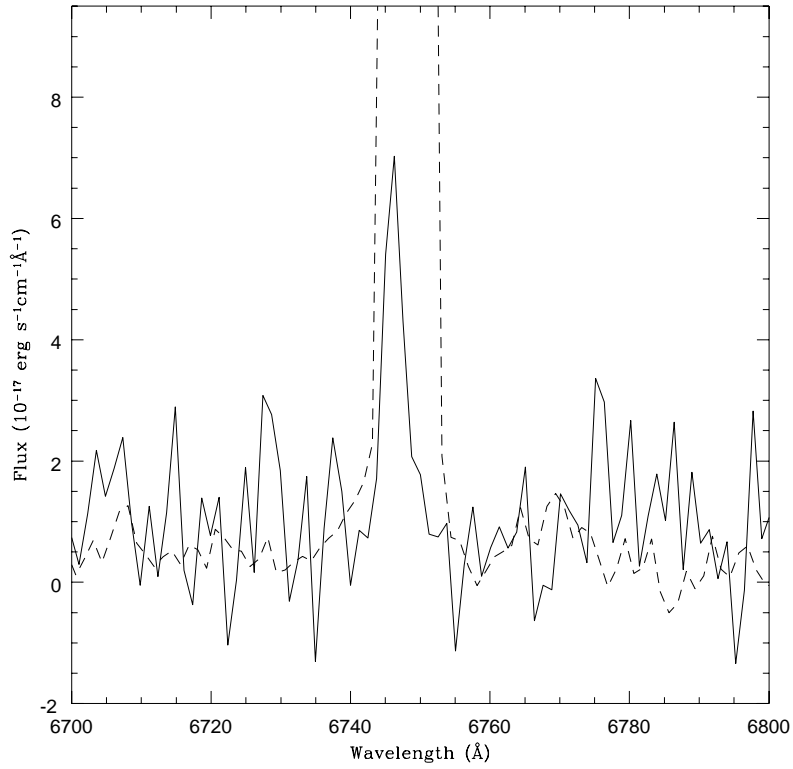


Fig. 5.— The solid line shows the spectrum of LSB-A634a_knot, spatially binned to increase the signal to noise ratio. The dashed line shows the spectrum of DRP-A634a around the $H\alpha$ line. The scale of the flux axis has been set to show the $H\alpha$ line of the knot component.

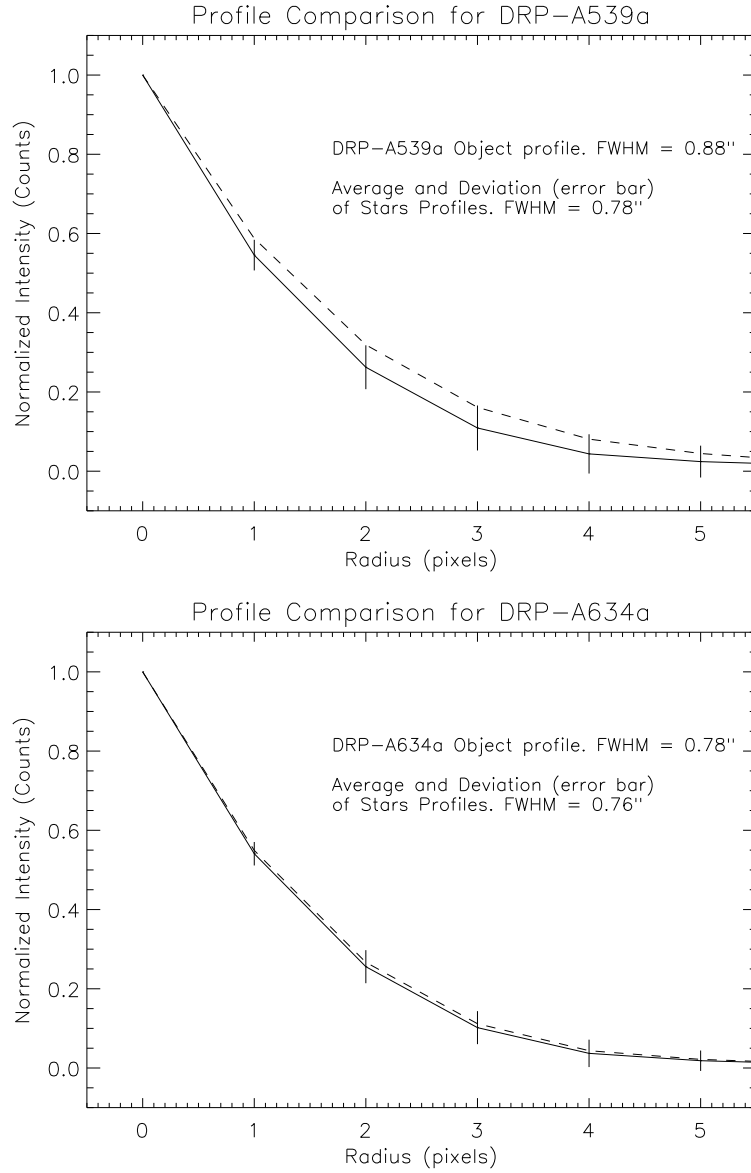


Fig. 6.— Radial profiles of DRP-A539a (upper panel) and DRP-A634a (lower panel) indicated by the dashed lines. The solid lines correspond to the stellar profiles averaged over a large number of stars for each frame.

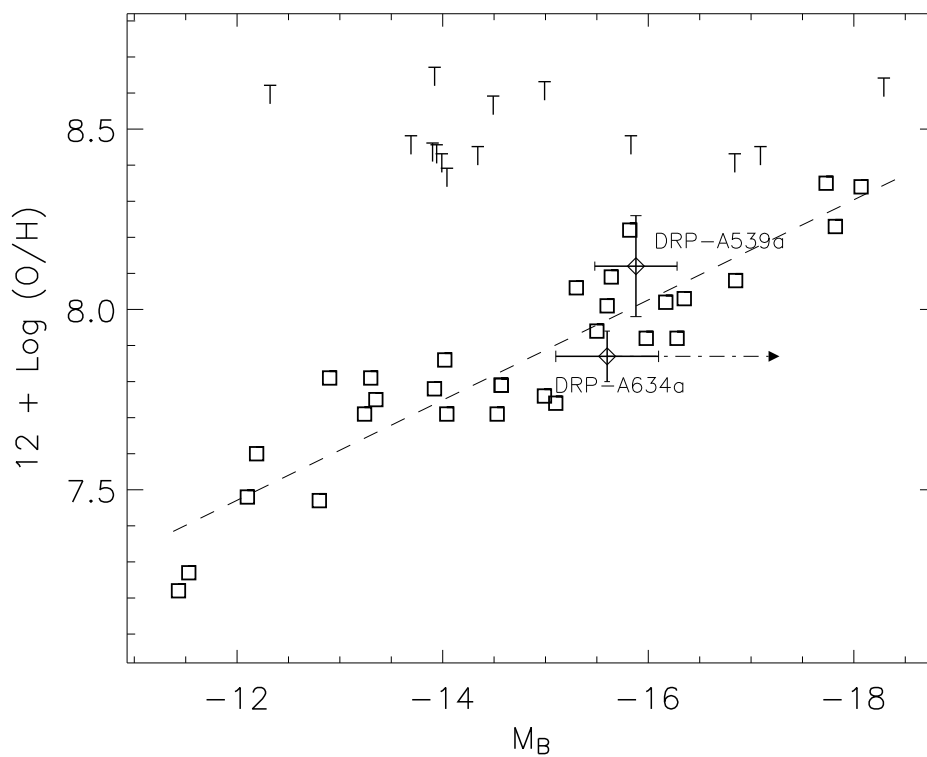


Fig. 7.— Luminosity-Metallicity relation for nearby dwarfs galaxies (open squares) adapted from Pilyugin, Vilchez, & Contini (2004). “T” symbols represent Tidal dwarfs (e.g. Kunth & Östlin 2000 and references therein). Our objects are overplotted as open diamonds with their error bars. The position of the luminosity M_B of the ensemble system LSB-A634a+DRP-A634a, is pointed out by the arrow.

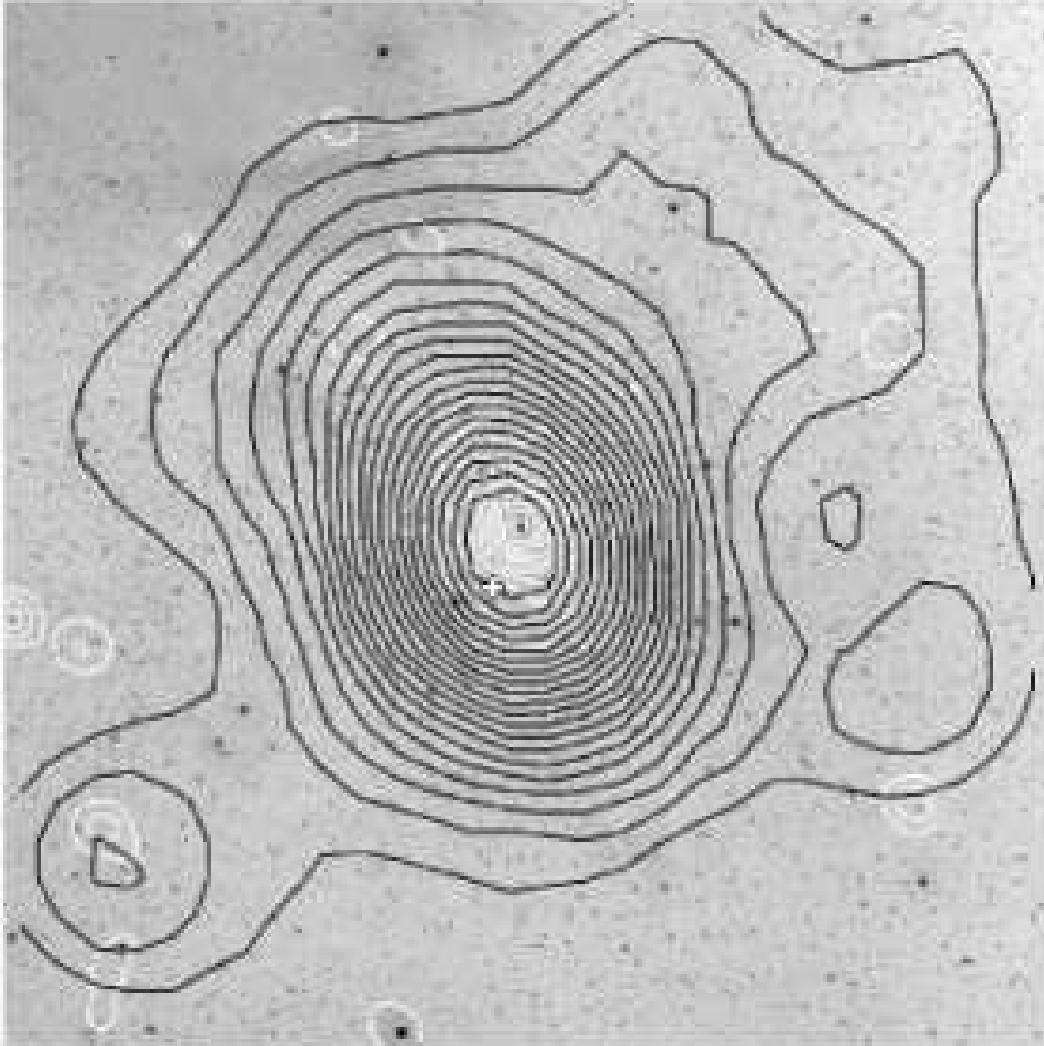


Fig. 8.— Abell 539 cluster DSS image with X-Ray ROSAT detection (white) and 2MASS galaxy spatial-density contours (black) overplotted (2x2 degrees) (relative units have been used for both contours parameters). Cross marks the position of the compact starburst galaxy relative to the cluster center. (North is to the top and East is to the left.)

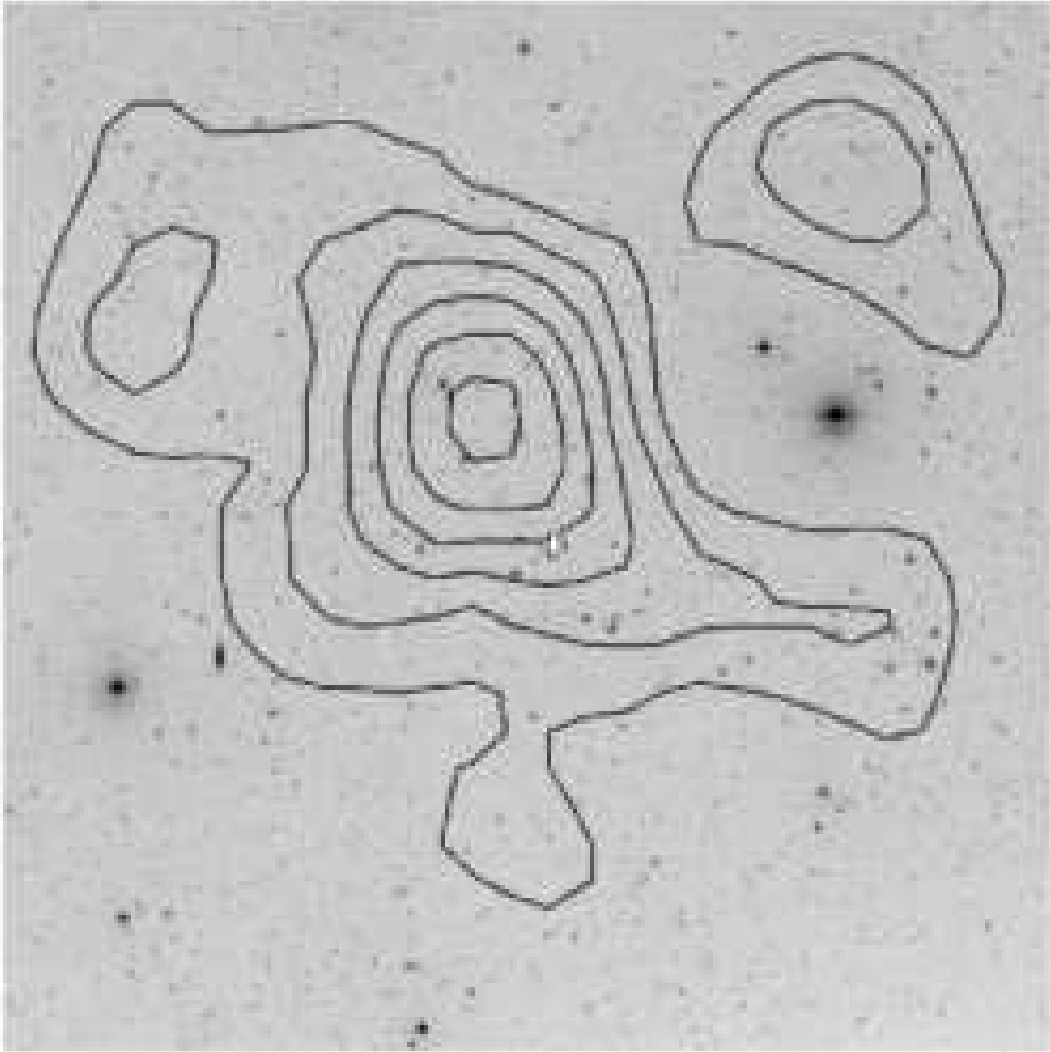


Fig. 9.— Abell 634 overview (2x2 degrees) with the 2MASS galaxy spatial-density contours (relative units, black). Cross marks the position of the compact dwarf galaxy detected (North is to the top and East is to the left). Because of the extreme low X Ray emission detected by ROSAT for this cluster, no X-Ray contours can be overplotted.